Formation and properties of composite coatings on a steel substrate

D. Jankura*, V. Bačová

Department of Technologies and Materials, Faculty of Mechanical Engineering, Technical University of Košice, Mäsiarska 74, 040 01 Košice, Slovak Republic

Abstract

The paper analyses the technology of plasma spraying of composite coatings onto a metal substrate. Al_2O_3-based ceramic materials with the addition of metallic and plastic components were used as the starting material. The subject of our research was investigation of the formation and certain properties of the above-mentioned composite coatings prepared using plasma-spray equipment with water arc stabilization. It is well known that such equipment shows high thermal capacity and temperature of the plasma jet. With this in mind, our main goal was to verify the behaviour of the plastic and metallic components of the powder in the process of forming the composite coating by plasma spraying. The obtained results have shown that plasma spraying with water arc stabilization is suitable for the formation of composite coatings of the ceramics-plastic and ceramics-metal types. These coatings show high quality and are suitable for many practical applications.

K e y   w o r d s: ceramic and composite coatings, plasma spraying, structure, properties

1. Introduction

Specific physical and chemical properties of ceramic materials predetermine them for application under extreme loading conditions. Ceramic materials show, in comparison with classical engineering materials, better properties mainly under thermal loading conditions, as well as better corrosion resistance, wear resistance, etc. One of possible technical applications of ceramic materials is the formation of ceramic coatings on metal structural (engineering) parts. Plasma spraying of powder ceramic materials is the basic production technology of such layers. Considering the heat capacity and the temperature, plasma spraying is a very suitable technology. The analysis of plasma spraying can be found in a number of articles [1–4]. Major advantages of the plasma spraying process, enabling its relatively wide use, include:

– wide range of sprayed materials, from metals with a high melting point, oxides and alloy combinations to plastics,

– negligible thermal influencing of the base material (up to 250 ℃), which guarantees the dimensional and structural stability of the substrate and makes it possible to use quite different materials, such as metals and their alloys, ceramics, concrete, wood, graphite, etc.,

– the possibility to form coatings whose thickness ranges from micrometres to millimetres, on both small and large surfaces,

– a high spraying output, especially for water-stabilized plasma spray units [5].

Plasma spraying is one of modern and productive spraying technologies. It is characterized by a very high concentration of heat and a high working temperature. Many various types of powder material spray equipment are used all over the world.

Plasma spray equipment consists of a number of individual units, the most important of them being a plasma torch. As an arc-stabilizing medium, plasma torches may use gas or water [6, 7].

For gas-stabilized torches, the influence of spraying parameters is much more complex. In addition to the current, the voltage and the velocity of the plasma jet, the quantity of the fed plasma, focusing and protective gas, the shape and design of nozzles and the

---

*Corresponding author: tel.: +421(0)55/6023514; fax: +421(0)55/6225186; e-mail address: daniel.jankura@tuke.sk
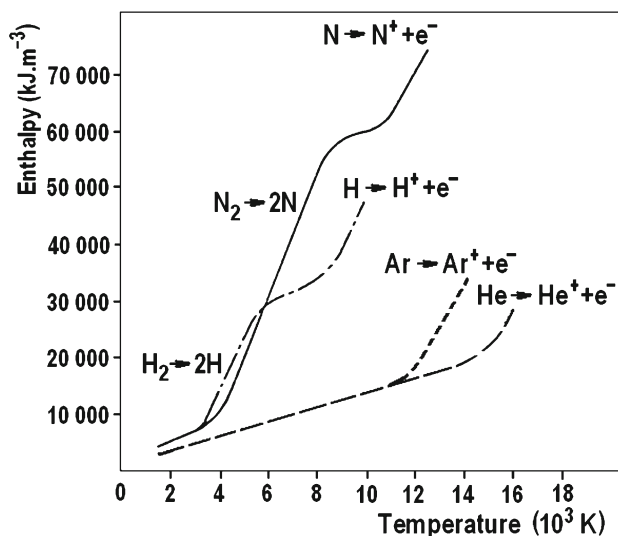
Fig. 1. Dependence of enthalpy on the plasma temperature for different plasma-forming gases.

diameter of the tungsten electrode play an important role. The properties of the generated plasma jet are strongly dependent on the used current. For effective heating of powder, the enthalpy, i.e. the energy content of plasma, plays a crucial role; see Fig. 1 [8]. Noble gases have a relatively high temperature at a relatively low enthalpy, whereas molecular gases H_2 and N_2 have a substantially higher enthalpy. As a result, even at a substantially lower temperature of these gases, it is possible to obtain plasma rich in energy, enabling sufficient heating of powder [7]. In the dependence of the used plasma gas, the temperature of gaseous plasma reaches 7–15 000 K, for helium up to 20 000 K [4, 9, 10].

A commercially available water-stabilized plasma torch consists of a specially shaped arc chamber, a rotary cooled copper anode and a graphite cathode. The mechanism of the arc plasma formation is based on the evaporation of the internal cylindrical wall of the water vortex surrounding the arc column. Evaporation is induced by the absorption of a fraction of the ohmic power of the arc. The ionized vapour inflows, and its heating creates an overpressure inside the arc chamber, which accelerates the plasma towards the exit orifice of the chamber. Thus, the arc properties are controlled by the processes influencing the evaporation from the wall and by the radial transport of energy from the arc centre towards the walls (inner surface of the water vortex). The resulting properties of the generated plasma jet are strongly dependent on the arc current. The temperature of the water-stabilized plasma arc reaches 30 000 K and more [11, 12].

The advantages and disadvantages of the systems with water (LP) and gas (GP) plasma stabilization

can be briefly summarized as follows [11]:

The GP system is suitable for forming high-quality small areas using special and/or expensive sprayed materials. A high price of plasma gases and a lower spraying output are disadvantages.

The LP system has a high intensity of spraying (in kg kW^{-1} h^{-1}), enabling the surface treatment of large areas as well as production of freestanding parts. A lower efficiency and complexity of the spray equipment are disadvantages of this system.

The main goal in the development of coatings is the increase of the service properties of products, material savings (especially of metal and rare materials), and extension of the product life. Classical materials are, despite continuing search for possibilities to further improve their properties, reaching the limits of their usability. Therefore, new material combinations are intensively developed, which would achieve the above-mentioned goals. In case of ceramic coatings, ceramics-plastic and ceramics-metal are suitable composite materials. The application of ceramic powders with a polymer addition has been documented for plasma spraying with gas arc stabilization [13]. However, the plasma temperature in a water arc stabilized unit is as much as two times higher than the temperature of gas plasma (30 000 K), so the question is how the doping material in the starting powder will behave in the spraying and coating formation process. Our primary goal was therefore to determine the behaviour of the plastic and metal components in the process of composite coating formation using plasma spraying with the water arc stabilization. These ceramic-based composite coatings were evaluated using the electron microscope and qualitative X-ray analysis and their microhardness was measured. Also the adhesion of the studied coatings was analysed, since this is a basic and crucial property of any functional coatings.

2. Experimental procedure

Experimental work was aimed at the investigation of the structure and selected properties of two types of Al_2O_3-based composite coatings:

a) Composite coatings with the addition of polymer, $Al_2O_3 + 3$ % $TiO_2 + 10$ % PTFE, designated AT3 + plastic. According to the manufacturer data, the granularity of the starting powder is 15–60 micrometres. For comparison of the properties of the composite coating and a ceramic coating on the same base, $Al_2O_3 + 3$ % TiO_2, was used, designated AT3. As an interlayer for improving adhesion and reducing a high difference between the thermal expansions of the coating and the substrate, a NiCr-based powder was used.

b) Composite coatings with the addition of a Ni-based metal component:

$Al_2O_3 + 5$ % K30 (vol.%), designated A5K

Al$_2$O$_3$ + 12 % K30, designated A12K
Al$_2$O$_3$ + 20 % K30, designated A20K.

K30 is a metal powder material with the following composition: Ni min. 90 %, Cr max. 2.5 %, Si max. 3.5 %, C max. 0.3 %, Fe max. 0.3 %. The granularity, given by the manufacturer as 40–90 micrometres, was confirmed by the sieve analysis. Mixed powders with the addition of a metal component were prepared by mechanical mixing under laboratory conditions.

The properties of composite coatings with the addition of a metal component were compared with ceramic Al$_2$O$_3$ coatings sprayed without an interlayer (designation A0) and with a NiCr interlayer (designation AM).

Prior to spraying, the basic substrate surface was pre-treated by mechanical blasting. Based on our previous results [14, 15], sharp-edged blasting material was chosen, i.e. corundum grit with the grain size d_z = 1.12 mm. The grain velocity during blasting was v = 80 m s^{-1}. Blasting was performed using a laboratory-blasting unit with the blast wheel of a Di-2 type.

Powders were deposited on the faces of steel rollers with the diameter of 25 mm, made of S235JRG2 material (STN 41 1375). Ceramic coatings of all the investigated types were deposited using plasma equipment with water arc stabilization WSP PAL-160, developed by the Institute of Plasma Physics AS CR in Prague, with the electric input of 160 kWh. The coating thickness ranged from 150 to 200 micrometres, the interlayer thickness from 60 to 70 micrometres.

The adhesion tests were performed on a tensile testing machine ZD 10 in compliance with the STN EN 582 Standard. A specimen with the applied coating is glued to a counterpart and clamped in the jaws of the testing machine. Then an increasing tensile stress is applied to the specimen, until the joint fails [16]. The value of the pull-off strength was determined as the average of five measurements.

The plasma-sprayed ceramic and composite ceramics-plastic coatings were subjected to a qualitative X-ray analysis, using an X-ray diffractometer URD 6. Evaluation was performed by the analysis of X-ray images. The microhardness of the coatings was measured in compliance with the STN ISO 4516 Standard, using a digital microhardness tester LECO LM 700 AT. The structure of the coatings was investigated using a scanning electron microscope TESLA BS 301. The chemical spectral analysis of the composite coatings with a metal component was performed on a microanalyser INCA.

3. Results and discussion

The main goal of our experiments was to confirm, using structural analysis, the presence of the plastic or metal component in the composite coating depos-
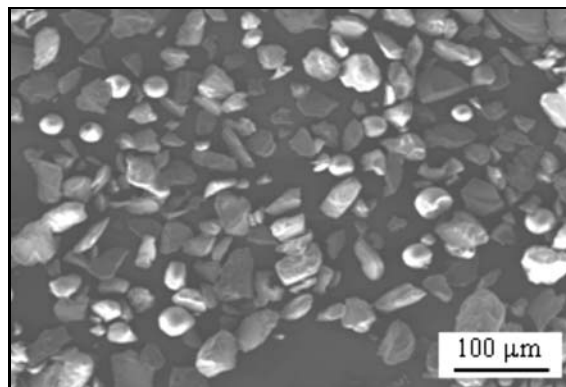

Fig. 2. Grains of the AT3 + plastic composite powder.

ited using plasma spraying equipment with water arc stabilization. Certain other properties were also measured, such as the thickness, the adhesion and the microhardness, enabling the comprehensive assessment of the investigated coatings.

3.1. Analysis of the composite coating with a plastic component

The starting powders were analysed in terms of their grain shape, and the microhardness of plastic grains was measured. The average microhardness of the plastic component in the composite powder was 579.2 HV 0.025. Figure 2 shows individual grains of the powder mixture. Figure 3a shows sharp-edged ceramic grains and Fig. 3b shows spherical plastic grains in the starting powder [17].

The influence of the polymer addition on the final hardness of the coatings was determined by measuring the microhardness on metallographic samples (Fig. 4). The average microhardness of the composite coating, determined from ten measurements, was 1104 HV 0.05; the microhardness of the ceramic coating was 1649.1 HV 0.05. However, the measurements showed a rather great scattering of the measured microhardness values. The composite AT3 + plastic coating showed the values from 560.6 to 1730.4 HV 0.05, while the values for the ceramic AT3 coating varied from 1483.6 to 1892.2 HV 0.05. The great scattering of the microhardness of the coating with a plastic component may be attributed to the presence of polymer particles in the coating. To verify this, additional 50 measurements were made and their results confirmed significant non-homogeneity in the coating structure. Six measurements (approx. 12 % of the total number of measurements) gave substantially lower values, which is in agreement with the share of plastic in the ceramic powder. These six values correspond with the microhardness of the plastic component in the starting powder (579.2 HV 0.025).

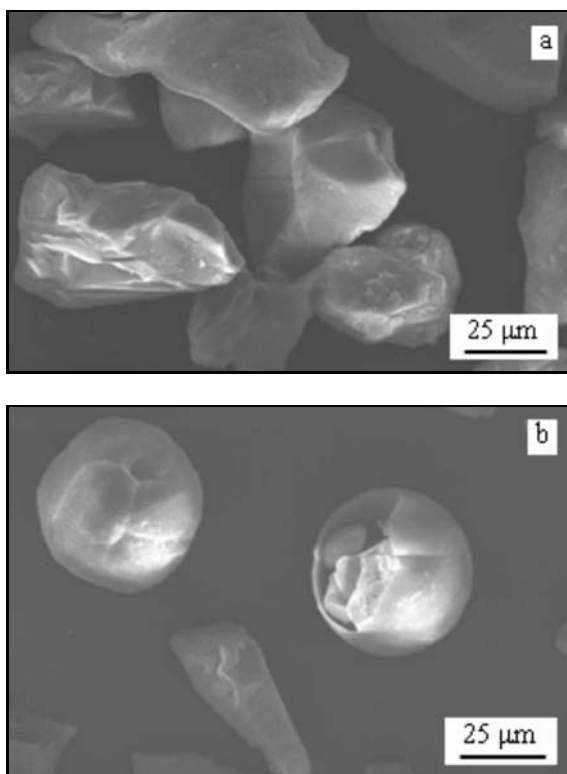The morphology of the fracture surfaces of the

Fig. 5. Fracture surface of ceramic coating AT3.

Fig. 3. Detail of particles of the initial AT3 + plastic powder: a) sharp-edged ceramic particles, b) spherical PTFE polymer particles.

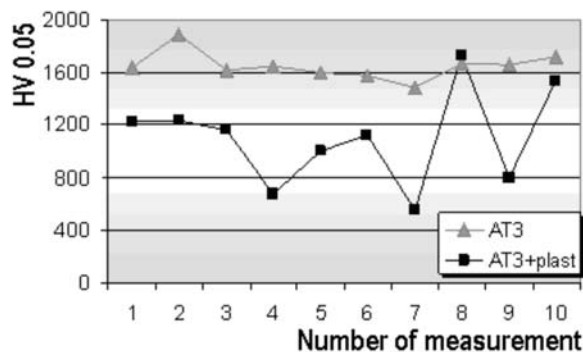Fig. 6. Fracture surface of composite coating AT3 + plastic.

Fig. 4. Microhardness of AT3 and AT3 + plastic.

show ductile properties and form very thin (less than 1 micrometre) membrane-like elements with irregularly shaped boundaries, which protrude from the fracture surface. This finding confirms the presence of a polymer component in the composite coating (during loading, a ductile fracture is predominantly formed).

Qualitative X-ray analysis was performed with the aim to identify the phase composition of the investigated coatings, their structural changes due to their application by high-temperature plasma, and to determine a possible influence of the amorphous polymer component of the composite coating on structural changes.

Figures 7 and 8 show diffractograms of the ceramic and composite coatings, obtained by qualitative X-ray analysis. There is a fundamental difference – in the shape and broadening of reflections (peaks) – between these two diffractograms. In the both coatings, a dominant α-Al_2O_3 phase (corundum) is present, which is a result of modification changes during the coating

investigated coatings is shown in Figs. 5, 6. Figure 5 shows the morphology of the Al_2O_3 + 3 % TiO_2 ceramic coating, which is of a typical sandwich nature. The layer contains relatively few voids, pores and other defects. Our most important finding when studying the fracture surfaces of the composite coating (Fig. 6) was the observation of amorphous phases on these surfaces. An arrow shows the polymer phase PTFE, which perfectly covers the surface of the contact layer of ceramic particles. Such matters are not present in the structure of the ceramic coating. The above-mentioned phases in the coating

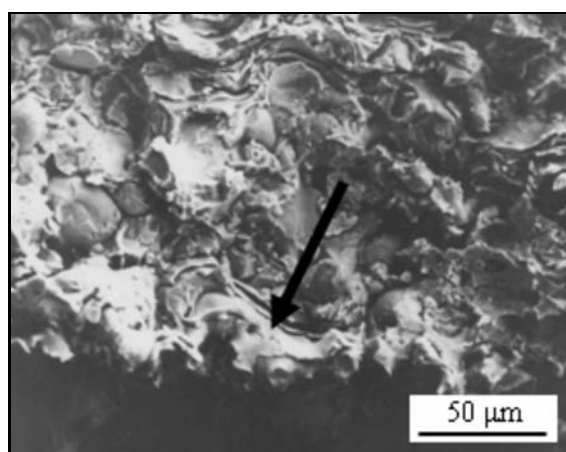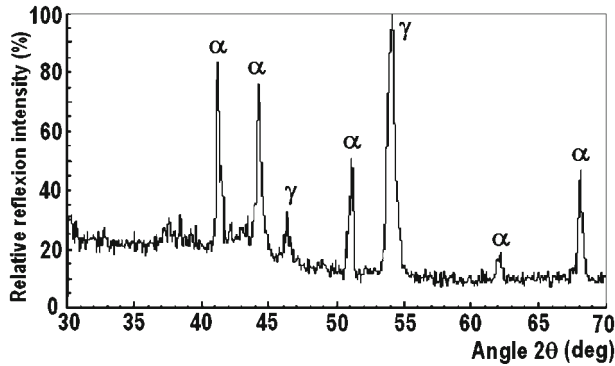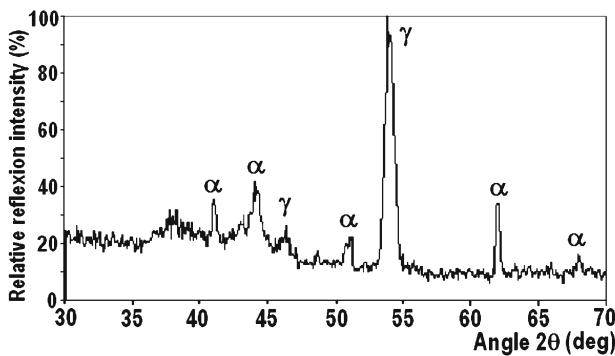Fig. 7. Diffraction diagram of the ceramic coating AT3, $\alpha = \alpha$-Al$_2$O$_3$, $\gamma = \gamma$-Al$_2$O$_3$.

Fig. 8. Diffraction diagram of the composite coating AT3 + plastic, $\alpha = \alpha$-Al$_2$O$_3$, $\gamma = \gamma$-Al$_2$O$_3$.
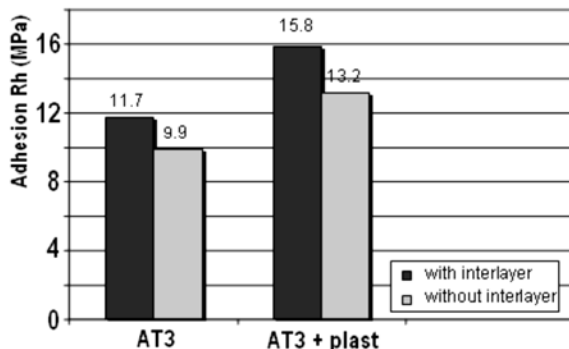

Fig. 9. Average values of adhesivity of coatings without and with interlayer.

cooling and solidification and whose presence is conditioned by the use of the stabilizing TiO$_2$ dopant. Also the γ-Al$_2$O$_3$ phase was identified, which dominates in Al$_2$O$_3$ coatings without stabilizing additives [18]. In the ceramic coating, the crystalline structure is more developed than in the composite one, which is documented by pronounced diffraction reflections. In the composite coating, the difference in crystallinity was seen, with not so pronounced diffraction maxima
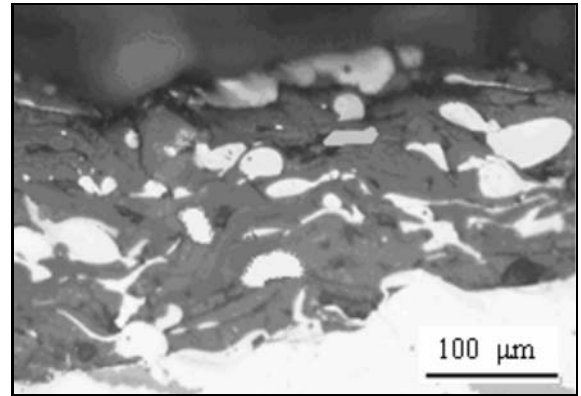

Fig. 10. The structure of the composite coating A12K.

of the α-Al$_2$O$_3$ phase. In the composite coating, a significant destruction of the α-Al$_2$O$_3$ phase takes place. The polymer component causes, due to its amorphous state, a decrease in crystallinity. The influence of the polymer components, especially of fluorine, on an atomic level, on the structure of the coating during its application by the plasma jet also cannot be excluded. Due to this the presence of polymer components causing amorphization may disturb the arrangement of planes in the coating crystalline structure, which is then manifested as a low and broad reflection on the diffractogram of the composite coating in question [19, 20].

The basic and crucial property of coatings is their adhesion strength or adhesiveness, since this property ensures the durability of the coating-substrate system, providing the protection of the substrate against various influences. The results of the adhesion tests of the investigated AT3 and AT3 + plastic coatings are shown in Fig. 9. For the both coatings, a positive influence of the ductile interlayer (NiCr) on adhesion of the coating to the substrate was confirmed; the increase of adhesiveness was about 15 % for the AT3 coating and up to 18 % for the composite AT3 + plastic coating. It follows from the comparison of adhesion of the both coatings that the composite coating shows about 25 % higher adhesion to the substrate than the ceramic one.

3.2. Analysis of the composite coating with a metallic component

The microhardness of the ceramic A0 (Al$_2$O$_3$) and composite A5K, A12K and A20K (Al$_2$O$_3$ + Ni) coatings was measured on metallographic samples. The structure of the composite coatings consists of a light phase and a dark phase, see Fig. 10. On each coating (and on each phase of the coating), five microhardness measurements were performed.

The results of these measurements are summarized in Fig. 11. The average microhardness of the ceramic
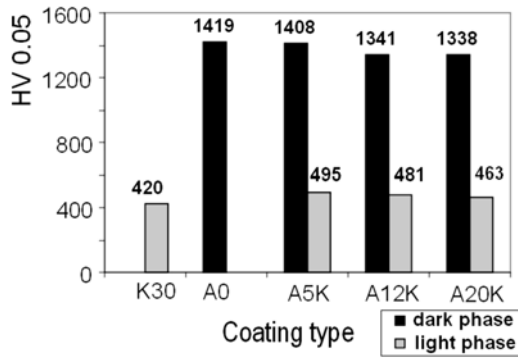
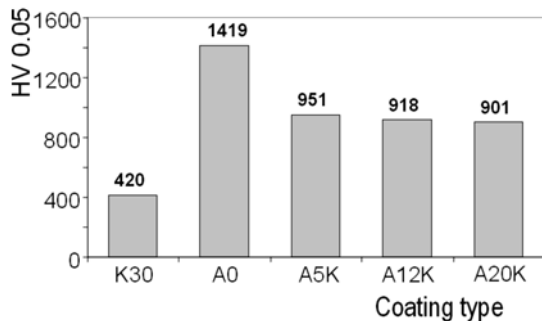Fig. 11. Microhardness of phases of individual coatings.

Fig. 12. The average value of microhardness of coatings.

A0 coating was 1419 HV 0.05, and that of the metal coating (of K30 powder) on the nickel base was 419.7 HV 0.05. The comparison of these values with the microhardness values of particular phases in the composite coatings leads to the conclusion that the dark phase corresponds to Al_2O_3 and the light phase to the nickel component [15]. The resulting microhardness of the composite coatings decreases with the increase of the metal component content, which is documented by the average microhardness values of the coatings, shown in Fig. 12.
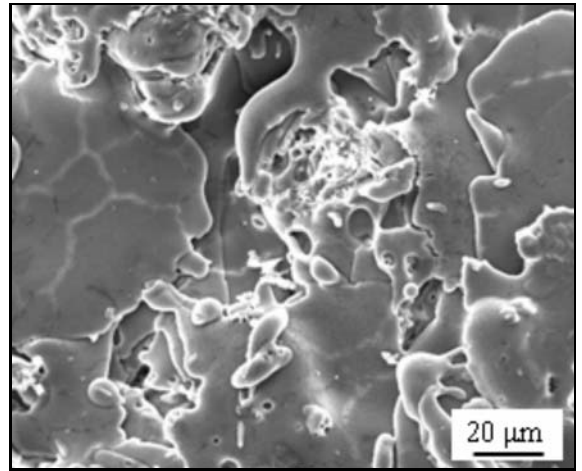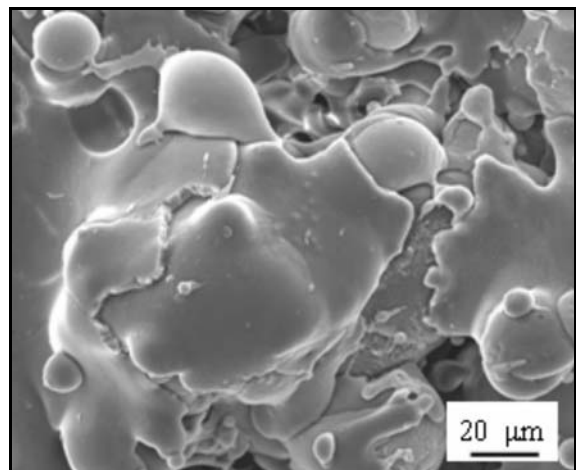

Fig. 13. Surface of the A0 coating (Al_2O_3).

Fig. 14. The surface of the composite coating A20K.

The structure of the Al_2O_3 coating is shown in Fig. 13. The surface of the coating is markedly heterogeneous and consists of individual disc-shaped splats.
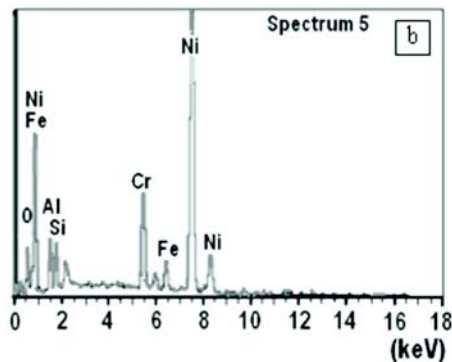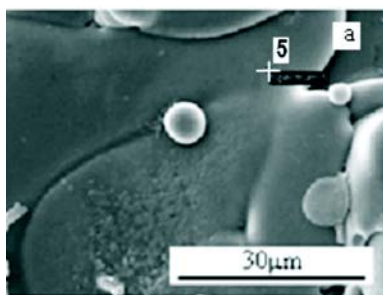

Fig. 15a,b. Spectral analysis of the surface of a slightly deformed particle.
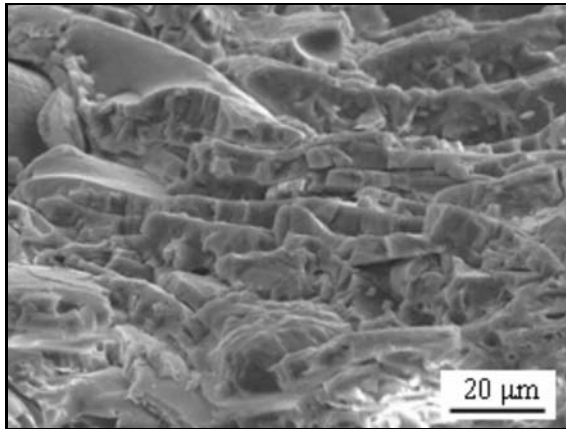
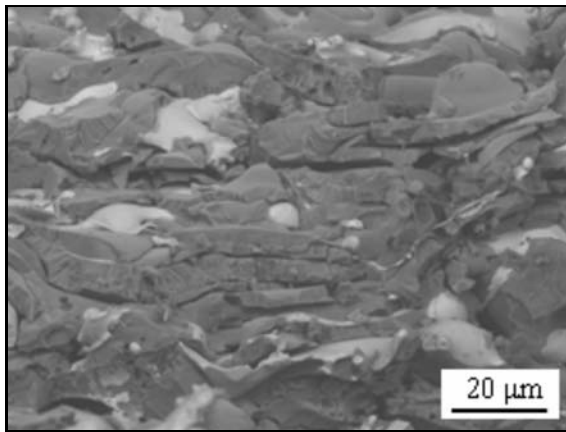Fig. 16. Fracture surface of the ceramic coating A0.

Fig. 17. Fracture surface of the ceramic coating A12K.

The particles (splats) are well spread and form a smooth surface. Overheated melted particles form local lobes from which small oval or spherical particles were separated. On the surface of splats, various defects, such as voids and cracks, can be observed, which were formed due to dilatation stresses in the coatings during cooling. The nature of the composite coating (Fig. 14) does not change in comparison with Al_2O_3. However, coating contains fewer defects (mainly cracks). On the surface, oval and only slightly deformed particles are observed, which are locally covered with completely melted ceramic Al_2O_3 splats. Microanalysis has shown that these slightly deformed particles are Ni-based particles, Fig. 15 a,b.

Figure 16 shows the lamellar arrangement of particles (disc-shaped splats) on the fracture surface of the ceramic coating. The coating consists of particles piled up in layers. This is a characteristic structure of the sandwich type. In the structure, some defects, such as pores, voids and cracks can be observed. Voids are formed after the impact of insufficiently
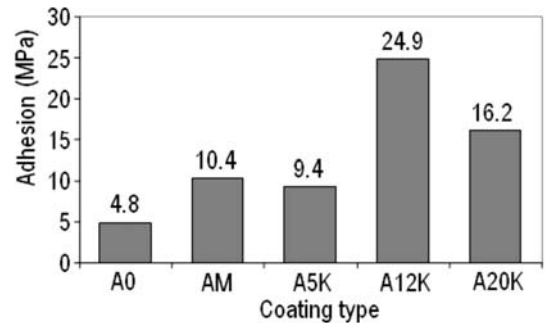

Fig. 18. Average adhesiveness values.

overheated particles, which do not completely cover the rough surface. Cohesion between individual splats would increase with the decrease of the number of defects (pores, voids and cold joints) and with the increase of the number of overlaps, wedged-in joints, etc.

Figure 17 shows the lamellar structure of the A12K composite coating, which is similar to that of the A0 ceramic coating, formed by aluminium oxide. However, the composite coating shows a lower number of defects (pores, voids, cracks). This leads to the increase of both the cohesive strength and the adhesion of the composite coating to the substrate. The coating also contains oval, slightly deformed metal particles, which are locally covered with perfectly molten ceramic Al_2O_3 splats.

Adhesiveness of the investigated coatings was determined by a pull-off test. The average values of adhesiveness of particular coatings are given in Fig. 18. It follows from the figure that the ceramic coating (Al_2O_3) without an interlayer shows the lowest adhesiveness. The interlayer has increased its adhesiveness twice. The addition of the Ni-based metal component (K30) to the basic Al_2O_3 powder has led to a substantial increase of adhesiveness of the composite coatings. The coating with 5 % addition of K30, formed without the interlayer, shows similar adhesiveness as the ceramic coating with the interlayer (AM). The composite coating with 12 % addition of K30 shows the highest adhesiveness, almost 25 MPa, which is a five-fold increase in comparison with the Al_2O_3 ceramic coating without the interlayer. For more exact determination of the Ni addition content at which maximum adhesion is achieved, it will be necessary to extend the experimental program.

These measurements have confirmed that the Ni addition in the Al_2O_3-based coatings significantly increases their adhesion to the substrate. This enables the application of composite coatings without using an interlayer and also contributes to a more efficient application of coatings. It can be assumed that the addition of a metal component increases the ductility of composite coatings and enables their utilization under

shock thermal stress conditions. Research in this field continues and its first results confirm these assumptions.

4. Conclusions

The evaluation of composite coatings with a plastic component brought the following conclusions:

– The microhardness values of the investigated coatings show great scattering, indicating significant non-homogeneity of the coating structure and confirming the presence of a polymer component in the coating.

– On the fracture surfaces of the coatings, the presence of very thin, membrane-like ductile particles was observed. This is a polymer phase in the coating, which fails through a ductile fracture during loading.

– Qualitative X-ray analysis of the composite coating has shown a marked decrease of the crystallinity of the ceramic phase due to the doping polymer component.

– A polymer component in composite coatings, both with and without an interlayer, increases the adhesiveness by up to 25 % when compared with the ceramic coating.

From the evaluation of the composite coatings with metal components, the following conclusions can be drawn:

– In the coating, a two-phase structure with different hardness values was identified. The average microhardness of the light phase was 479 HV 0.05, while that of the dark phase was 1362 HV 0.05. We can conclude from this that the light phase is based mainly on the K30 metal component and the dark phase is based on Al_2O_3. The total microhardness of the composite coatings decreases with the increase of the Ni-based K30 metal component content.

– The K30 metal component in the composite A5K, A12K and A20K coatings increases their adhesion to the basic substrate without an interlayer. As little as 5 % addition of the K30 metal component leads to the adhesiveness value, which is comparable to that of the ceramic coating with an interlayer. The highest adhesiveness, almost 25 MPa, was observed for the A12K composite coating. This is a substantial increase when compared with both the AM ceramic coating with an interlayer (about 2.5-times) and with the A0 ceramic coating without an interlayer (about 5-times).

Based on the performed experiments and the analysis of their results it can be stated that the technology of plasma spraying using equipment with water arc stabilization is suitable for producing composite coatings with plastic or metal dopants. Coatings produced using such a technology show qualitatively better properties and are suitable for various practical applications.

References

[1] MATEJKA, D.—BENKO, B.: Plazmové striekanie kovových a keramických práškov. Bratislava, Alfa 1988 (in Slovak).

[2] CHASUJ, A.—MOGIRAKI, O.: Naplavka i napylenije. Moskva, Mašinostrojenije 1985 (in Russian).

[3] SURYANARAYANAN, R.: Plasma Spraying: Theory and Applications. London, CNRS 1993.

[4] AMBROŽ, O.: Zváranie, *42*, 1993, p. 152.

[5] CHRÁSKA, P.—DUBSKÝ, P.—KOLMAN, B.—ILAVSKÝ, J.—FORMAN, J.: Journal of Thermal Spray Technology, *4*, 1992, p. 3016.

[6] HRABOVSKÝ, M.—KONRÁD, M.—KOPECKÝ, V.—SEMBER, V.: IEEE Transactions on Plasma Science, *35*, 1997, p. 833.

[7] SOLOLENKO, O. P.: Thermal Plasma Torches and Technologies. Cambridge, Cambridge International Science Publishing 2000.

[8] BURNHORN, F.—WIENECKE, R.: Z. Physik. Chem., *215*, 1960, p. 269.

[9] TURŇA, M.: Špeciálne metódy zvárania. Bratislava, Alfa 1989 (in Slovak).

[10] AUBRECHT, V.: Technické aplikace plazmatu. Brno, Vutium 2003 (in Czech).

[11] CHRÁSKA, P.—HRABOVSKÝ, M.: In.: Proc. Int. Thermal Spray Conf. & Exposition 1992. Ed.: Berndt, C. C. Materials Park, OH, ASM Int. 1992, p. 81.

[12] DUBSKÝ, J.—KOLMAN, B.—FORMAN, J.: In.: I. národní konference o plazmových a žárových nástřicích. Eds.: Musil, J., Kubíček, J., Korčák, S. Brno, CONMET 1994, p. 150.

[13] BÜLTMANN, F.—HARTMANN, S.: Vlastnosti termicky nastřikovaných vrstev obsahujících PTFE. Svařák.cz, 2006, http://www.svarak.cz/c/cz-2/vlastnosti-termicky-nastrikovanych-vrstev-obsahujicich-ptfe.htm (1.2.2009).

[14] BAČOVÁ, V.—KNIEWALD, D.—CTIBOR, P.—NEUFUSS, K.: Acta Mechanica Slovaca, *7*, 2003, p. 17.

[15] JANKURA, D.—PAPCUN, P.: Acta Mechanica Slovaca, *11*, 2007, p. 108.

[16] KNIEWALD, D.—BAČOVÁ, V.—ŠEFARA, M.: Niku-Lari – Advances in surface treatment VI. Oxford, GB, Pergamon Press Ltd. 1988, p. 174.

[17] POĽAK, J.: Formation and properties study of new composite plasma sprayed materials. [PhD. Thesis]. Košice, Faculty of Mechanical Engineering, Technical University of Košice 2006.

[18] KUDINOV, V.—IVANOV, V.: Nanesenije plazmoj tugoplavkich pokrytij. Moskva, Mašinostrojenije 1981 (in Russian).

[19] FROHLICH, L.—FROHLICHOVÁ, M.—JANÁK, G.—LOHAY, T.: Metallurgija, *39*, 2000, p. 119.

[20] VOLENÍK, K.—SCHNEEWEISS, O.—LEITNER, J.—KOLMAN, B.—PÍSAČKA, J.: Kovove Mater., *46*, 2008, p. 17.